Journal of Neuroscience Methods 292 (2017) 20–29

Contents lists available at ScienceDirect

Journal of Neuroscience Methods

journal homepage: www.elsevier.com/locate/jneumeth

Prolonged striatal disinhibition as a chronic animal model of tic disorders

Esther Vinner, Michal Israelashvili, Izhar Bar-Gad*

Gonda Multidisciplinary Brain Research Center, Bar Ilan University, Ramat Gan, Israel

HIGHLIGHTS

- The chronic model is an adaptation of the acute striatal disinhibition model.
- Mini osmotic pumps were used for prolonged bicuculline infusion to the striatum.
- Motor tics were expressed throughout the infusion period (multiple days).
- Tics were accompanied by stereotypical LFP spikes throughout the period.
- Neuronal activity around the tic time was stereotypic and stable across days.

ARTICLE INFO

Article history:
Received 27 September 2016
Received in revised form 20 January 2017
Accepted 3 March 2017
Available online 6 March 2017

Keywords:
Tourette syndrome
Motor tics
Basal ganglia
Striatum
Osmotic pump

ABSTRACT

Background: Experimental findings and theoretical models have associated Tourette syndrome with abnormal striatal inhibition. The expression of tics, the hallmark symptom of this disorder, has been transiently induced in non-human primates and rodents by the injection of $GABA_A$ antagonists into the striatum, leading to temporary disinhibition.
New method: The novel chronic model of tic expression utilizes mini-osmotic pumps implanted subcutaneously in the rat's back for prolonged infusion of bicuculline into the dorsolateral striatum.
Results: Tics were expressed on the contralateral side to the infusion over a period of multiple days. Tic expression was stable, and maintained similar properties throughout the infusion period. Electrophysiological recordings revealed the existence of tic-related local field potential spikes and individual neuron activity changes that remained stable throughout the infusion period.
Comparison with existing methods: The striatal disinhibition model provides a unique combination of face validity (tic expression) and construct validity (abnormal striatal inhibition) but is limited to sub-hour periods. The new chronic model extends the period of tic expression to multiple days and thus enables the study of tic dynamics and the effects of behavior and pharmacological agents on tic expression.
Conclusions: The chronic model provides similar behavioral and neuronal correlates of tics as the acute striatal disinhibition model but over prolonged periods of time, thus providing a unique, basal ganglia initiated model of tic expression. Chronic expression of symptoms is the key to studying the time varying properties of Tourette syndrome and the effects of multiple internal and external factors on this disorder.

1. Introduction

Tic disorders (TDs) are characterized by the occurrence of motor and/or vocal tics which are defined as sudden, rapid, recurrent, non-rhythmic movements or sounds (American Psychiatric Association, 2013). TDs are classified according to tic type and persistency into (1) provisional (transient) TD, (2) persistent (chronic) TD, and (3) Tourette syndrome (TS). Tics typically appear during childhood, wax and wane over multiple timescales and in most cases decrease or even disappear in early adulthood (Leckman et al., 1998; McNaught and Mink, 2011). During this period, tic expression is modulated by behavioral states and environmental factors (Silva et al., 1995). The neural mechanism underlying the disorder remains unclear but has been associated with various dysfunctions of the basal ganglia (BG) in multiple experimental (Singer

Abbreviations: ACSF, artificial cerebrospinal fluid; BG, basal ganglia; FSI, fast spiking interneuron; GP, globus pallidus; LFP, local field potential; PTTH, peri-tic time histogram; SPN, spiny projection neuron; TD, tic disorder; TS, Tourette syndrome.

* Corresponding author.
E-mail address: izhar.bar-gad@biu.ac.il (I. Bar-Gad).

http://dx.doi.org/10.1016/j.jneumeth.2017.03.003
0165-0270/

and Minzer, 2003; Abelson et al., 2005; Kalanithi et al., 2005; Baym et al., 2008) and theoretical (Albin and Mink, 2006; Leckman et al., 2006) studies. Within the basal ganglia, reduced inhibition within the striatum, the primary input nucleus, has most explicitly been associated with tic expression (Peterson et al., 2003; Kalanithi et al., 2005; Albin and Mink, 2006; Kataoka et al., 2010).

GABAergic inhibition plays a key role in striatal function: spiny projection neurons (SPNs), which make up roughly 95% of the population, form a large collateral network within the striatum (Preston et al., 1980). Multiple types of GABAergic interneurons, including the fast spiking interneurons (FSIs) exert powerful inhibition on the SPNs (Tepper et al., 2004). Finally, recurrent GABAergic input from the arkypallidal neurons of the globus pallidus (GP) innervates the striatum (Mallet et al., 2012).

Functional models of the cortico-basal ganglia pathway suggest that during tic disorders, abnormal striatal inhibition leads to the formation of a focal area in the striatum which is abnormally overactive. This striatal area, in turn, inhibits a subset of downstream basal ganglia neurons which in turn disinhibit the thalamus, leading to the generation of the unwanted movements by the cortex (Mink, 2001 Albin and Mink, 2006). In line with this hypothesis, local disinhibition in the striatum of experimental animal models using acute microinjections of $GABA_A$ antagonists such as bicuculline and picrotoxin (Marsden et al., 1975; Tarsy et al., 1978) has led to transient formation of tics in both rodents (Bronfeld et al., 2013b; Pogorelov et al., 2015) and primates (McCairn et al., 2009, 2016). The location and type of the tics induced by the striatal disinhibition depends on the injection site within the striatum. Injections in the motor striatum lead to motor tics whose location is somatotopically organized, while injections in the limbic striatum (i.e. nucleus accumbens) lead to vocal tics (Bronfeld et al., 2013b; McCairn et al., 2016). Individual tic timing was shown to be dependent on the summation of the excitatory (glutamatergic) inputs to the striatum (Israelashvili and Bar-Gad, 2015). Electrophysiological recordings during tic expression have revealed the existence of a slow fluctuation of the local field potential (LFP) around the time of individual tics, termed "LFP spikes" (Muramatsu et al., 1990; McCairn et al., 2009). In addition, phasic tic-related firing rate changes were reported to appear throughout the cortico-basal ganglia loop (McCairn et al., 2009; Bronfeld et al., 2011; Israelashvili and Bar-Gad, 2015).

The acute model of tic expression produced by a temporary blockade of $GABA_A$ based synaptic transmission leads to transient periods of roughly one hour of tic expression. This is useful when studying short term phenomena such as the spatial and temporal attribution of individual tics. However, to investigate the fluctuation of tic expression over time and its modulation by behavior and/or pharmacological agents, tics must be studied over longer periods. Here we present a chronic tic model which preserves the key properties of the acute striatal disinhibition experimental animal model but extends the time course of tic expression to many days.

2. Methods

2.1. Animals

Six adults rats (Long-Evans, females) weighing 285 ± 25 g (mean $\pm$ SD) were used in this study. The rats were maintained under conditions of controlled temperature and humidity, in a 12 h light/dark cycle, with free access to food and water. The rats were monitored daily and assessment of pain and distress symptoms was performed using a standard scoring system (Morton and Griffiths, 1985; Scharmann, 1999). The rats' body weight and overall condition were checked at least twice daily. There was no significant weight loss compared to standard post-operational states and the weight loss did not exceed 10% of the original weight in any of the animals. The overall evaluation of the condition did not reach to a termination criterion in any of the animals. All procedures were approved and supervised by the Institutional Animal Care and Use Committee (IACUC) and were in accordance with the National Institutes of Health Guide for the Care and Use of Laboratory Animals and the Bar-Ilan University Guidelines for the Use and Care of Laboratory Animals in Research. The study was approved by the National Committee for Experiments in Laboratory Animals at the Ministry of Health.

2.2. Surgery

An injection cannula (stainless steel 30 gauge tube) curved at 90° was attached to a catheter (Polyethylene (PE-10) tubing; external diameter: 0.61 mm) which was attached to a mini-osmotic pump (ALZET pumps, DURECT Corporation) through an alcohol controlled tubing adapter (CMA Microdialysis) (Fig. 1A). The cannula was implanted to enable micro infusion into the dorsolateral striatum (injection target: AP, 1.0 mm; ML, 2.5 mm; DV, 5 mm) (Fig. 1B) (Paxinos and Watson, 2007). The mini-osmotic pump (4 animals: ALZET Model 2001, volume 200 μl, release rate 1 μl/hr, 7 days; 2 animals: ALZET Model 2002, volume 200 μl, release rate 0.5 μl/hr, 14 days) and the catheter were filled, separately, with artificial cerebrospinal fluid (ACSF containing (in mM): 145 NaCl, 15 Hepes, 2.5 KCl, 2MgCl2, 1.2 CaCl2, pH 7.4 with NaOH) or bicuculline methiodide (Sigma-Aldrich) dissolved in ACSF (final concentration of 1 μg/μl for ALZET model 2001 or 2 μg/μl for ALZET model 2002) for at least 4–6 h before the implantation, then connected together and primed in a saline bath at 37° C. Following the cannula implantation, the pump was inserted into a subcutaneous pocket on the rat's back. Custom-made movable bundles of 16 Formvar-insulated nichrome microwires (25 μm diameters) (Yael et al., 2013) were implanted, targeting the dorsolateral striatum (AP, 0.25 mm; ML, 2.75 mm; DV, 4 mm) or the globus pallidus (AP, −0.95 mm; ML, 3.2 mm; DV, 5 mm) for neuronal recording (Fig. 1C). The pump was replaced in some animals, either to switch between ACSF and bicuculline (2 animals) or to extend the infusion period of bicuculline (1 animal, data not shown).

2.3. Experimental sessions

Initial implantation of a bicuculline filled pump (4 animals) led to tic expression commencing during the first day after surgery. In the case of an initial ACSF infusion (2 animals), the rats had a recovery period of 5–7 days followed by a bicuculline pump exchange and an additional day before recordings to allow full recovery. Daily experiments in the chronic model consisted of 1–2 recording sessions, each lasting 100 min. Each session was analyzed by sampling 5 non-continuous segments of 2 min each (Fig. 1D).

2.4. Behavioral data

Identification of the rats' behavioral states and their relation to tic expression was achieved via manual analysis of a single camera video stream (30/60 frames/s; HC-W850, Panasonic). Video based observation specified five behavioral states: (1) Exploration; the rat engaged in locomotion, or extensive sniffing. (2) Quiet waking; the rat was awake and immobile. (3) Feeding; the rat was eating or drinking. (4) Grooming; the rat presented stereotypic grooming behavior. (5) Eyes closed; the rat displayed a stereotypic posture of sleep combined with slowed breathing. Due to the limitation of using only visual indicators, this cannot be determined to be a state of sleep (Gervasoni et al., 2004).

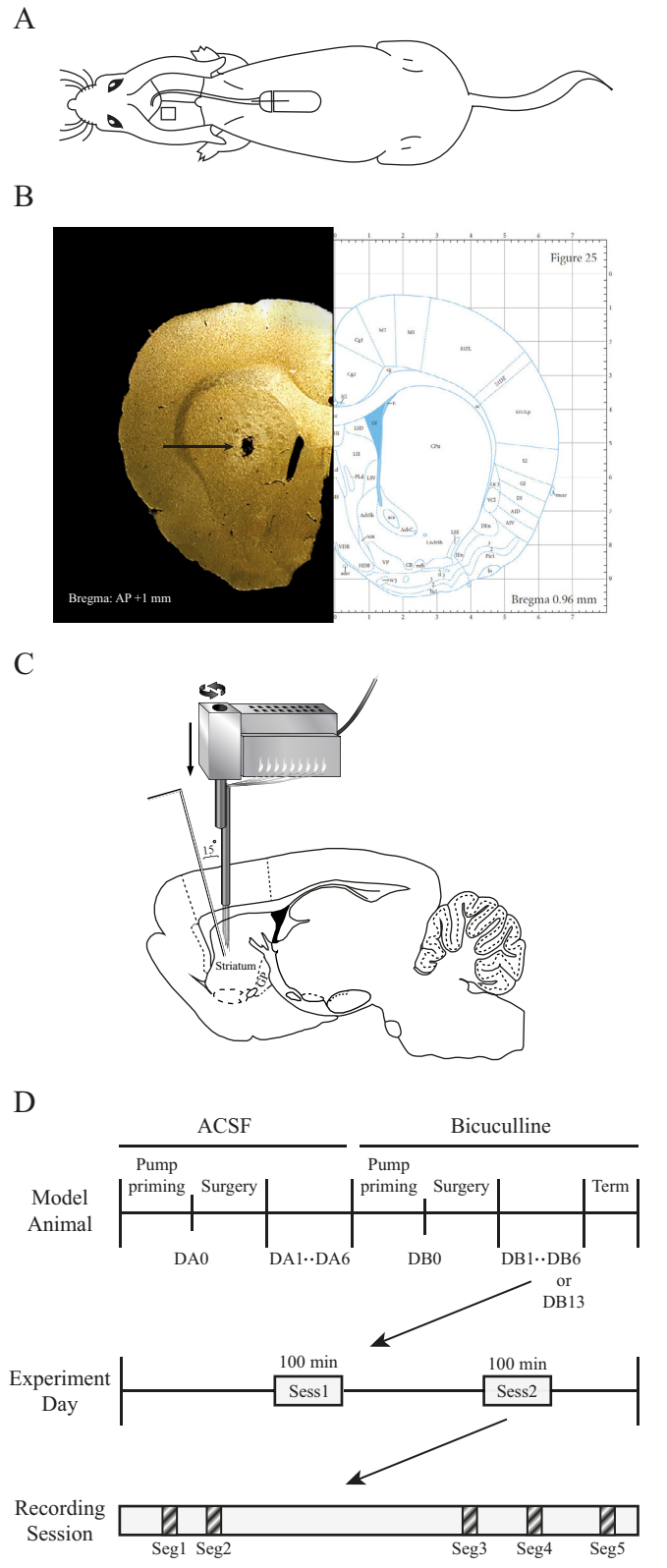

Fig. 1. Experimental setup. (A) A mini-osmotic pump implanted subcutaneously in the back of a rat with a catheter attachment leading to a cannula targeting the left dorsolateral striatum. The recording array targets the striatum or the GP of the same hemisphere (square area). (B) Coronal section of the left hemisphere from an infused rat (left). The black arrow points to the infusion site. The equivalent stereotaxic figure (right) taken from the Paxinos & Watson rat brain atlas (Paxinos and Watson, 2007). (C) Illustration of the cannula and the recording array, and their location in the left dorsolateral striatum. (D) The timeline of the experiment includes alternating periods of 7 days of ACSF followed by 7 (or 14) additional days of bicuculline infusion. Within a single session (100 min), tic dynamics and neural correlates were analyzed from 5 non-continuous segments (2 min each).

2.5. Neurophysiological data

During the experimental sessions, the neurophysiological data were recorded continuously while the animal was awake and moving freely in the recording chamber, and was connected to the recording system. The electrode signal was amplified (*200), wide bandpass filtered (0.5–10000 Hz, 4 pole Butterworth filter), and sampled continuously at 44 kHz (Alpha-Lab SNR, Alpha-Omega Engineering). The recorded data were pre-processed offline to extract the LFP and single unit spike trains which were used for additional analyses. The signal was sorted offline (Offline Sorter, version 2.8.8; Plexon) into multiple single-unit spike trains. The neurons were divided into three different types (SPN, FSI, and GP) according to their recording location, firing rate and waveform shape. Tonically active neurons and other neurons that did not belong to these clusters were excluded from the database. All additional analyses were performed using custom-written MATLAB code (V2012B; MathWorks). The LFP signal was obtained from the recorded data using a low-pass filter (25 Hz, 6 pole zero-phase forward-backward Butterworth filter). LFP spikes were detected using a semi-automatic threshold-crossing method on the LFP signal. Tic-related neural activity was assessed with a peri-tic time histogram (PTTH), using the individual tic times as a reference point. The PTTH was calculated using 1 ms bins and was smoothed with a Gaussian window (SD of 10 ms). All the neural data analysis was performed on the waking states of the rat, excluding feeding and grooming in order to avoid artifacts.

Throughout the manuscript, the results are compared to data from the acute model of tic expression as described in detail elsewhere (Israelashvili and Bar-Gad, 2015). All the results are expressed as the mean ± SD.

3. Results

Prolonged infusion of bicuculline was achieved via a mini-osmotic pump implanted subcutaneously in the rats' backs (Fig. 1A). Bicuculline (or ACSF) was infused into the dorsolateral striatum through a catheter attached to a cannula (Fig. 1B).

3.1. Chronic tic expression

Infusion of bicuculline led to ongoing motor tics on the contralateral side of the infusion, which could be identified via high-speed video monitoring. Tics appeared simultaneously or separately in three isolated muscle groups of the head, jaw and forelimb. Tics began during the first day after bicuculline pump implantation and were expressed for multiple days. During this period, their rate changed over multiple time frames; within a time span of 24 h, tics waxed and waned while the rat presented the typical repertoire of behaviors, such as exploration, quiet waking, grooming, feeding and eyes closed (see Supplementary Movie 1). Video based tic detection rate was highest at the quiet waking state, and was lowest when the rat's eyes were closed (Fig. 2A).

Tics were associated with the appearance of slow changes in the LFP ("LFP spikes") throughout the striatum and GP (Fig. 2B). The high fidelity of the appearance of LFP spikes during tics enabled the detection of tics with high temporal accuracy using the occurrences of these LFP spikes. In order to minimize the impact of the spontaneous behavior on the results, the analyzed data represents only the awake state of the animals during stages of quiet resting or exploration. Tics were analyzed from 21 experimental sessions in 6 animals. The tic rate in each day was calculated using 5 non-contiguous segments (Fig. 3A). The tic rate fluctuated over short time scales (minutes) (Fig. 3B); while maintaining largely similar histograms of the inter-tic intervals (ITIs) across days (Fig. 3C).

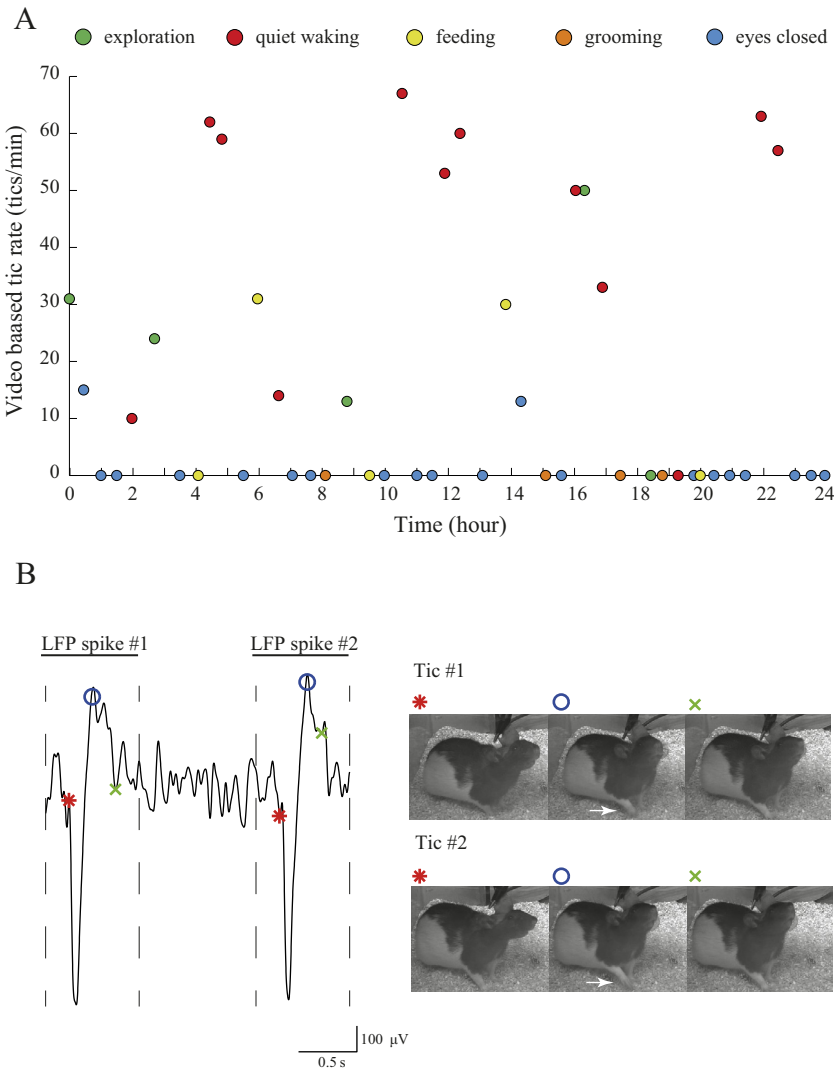

Fig. 2. Behavioral states during tic expression. (A) Video based tic rate during different behavioral states (exploration, quiet waking, feeding, grooming, and eyes closed), within a single day of the bicuculline infusion period. Tic rate was sampled every 31.9 ± 8.5 min during a continuous 24 h period. (B) Stereotypic LFP deflections (left) around the time of the tic which were identified using high-speed video monitoring (right). A single video frame of the initiation, maximum contraction and termination time of the tic was detected and marked on the LFP signal (red asterisk, blue circle and green X, respectively). The white arrow points to the forelimb tic location. (For interpretation of the references to colour in this figure legend, the reader is referred to the web version of this article.)

Changes in tic rate were observed both between sessions, within the same animal, and across animals (Fig. 3D). The chronic model extended the time course documented by the existing acute model from tens of minutes (Fig. 3E) to multiple days of tic expression, while preserving the same non-rhythmic tic pattern of appearance (Fig. 3F). Tics were more frequent in the chronic model (typically 40–60 tics/min) than in the acute model (typically 20–30 tics/min). Occasional short tetanic LFP episodes occurred resembling those observed in the acute primate and rodent models (McCairn et al., 2009; Pogorelov et al., 2015). For control purposes, we infused ACSF in two animals, which did not cause tic expression.

3.2. Neurophysiological correlates of tics – local field potential

The LFP spikes were highly stereotypic in shape over short time scales (minutes). The shape of the LFP spikes and the stability of their shape were comparable to the LFP spikes seen in a single session in the acute model although their magnitude was typically smaller (Fig. 4A). In the chronic model, LFP spikes were observed over multiple days, while maintaining their shape over multiple segments (Fig. 4B). The preservation of the LFP spike shape within a single animal over multiple days contrasts with the changes observed in the LFP spike shape in the acute model within a single animal between different sessions (fig. 4C). The stereotypic shape led to smaller variability and increased correlations between the mean LFP spikes shape for different sessions in the same animal in the chronic model (mean correlation coefficient between sessions within the same animals of the chronic model: 0.992 ± 0.006; acute model: 0.917 ± 0.047; Fisher z-transformation, $p < 0.01$). The LFP spike shape differed across animals displaying chronic tics (Fig. 4D). These differences were similar to those observed between acute model animals (mean correlation coefficient across animals of the chronic model: 0.046 ± 0.679; acute model: 0.086 ± 0.514, data not shown; Fisher z-transformation $p > 0.05$).

3.3. Neurophysiological correlates of tics – single neuron activity

We recorded the activity of 66 neurons from 6 animals during 12 experimental sessions. The neurons were identified as striatal spiny projection neurons (SPNs) (n = 29), fast spiking interneurons (FSIs) (n = 24) and GP neurons (n = 13). Most of the recorded neurons (SPN, 27/29, 93%; FSI 24/24, 100%; GP 9/13, 69%) displayed tic-

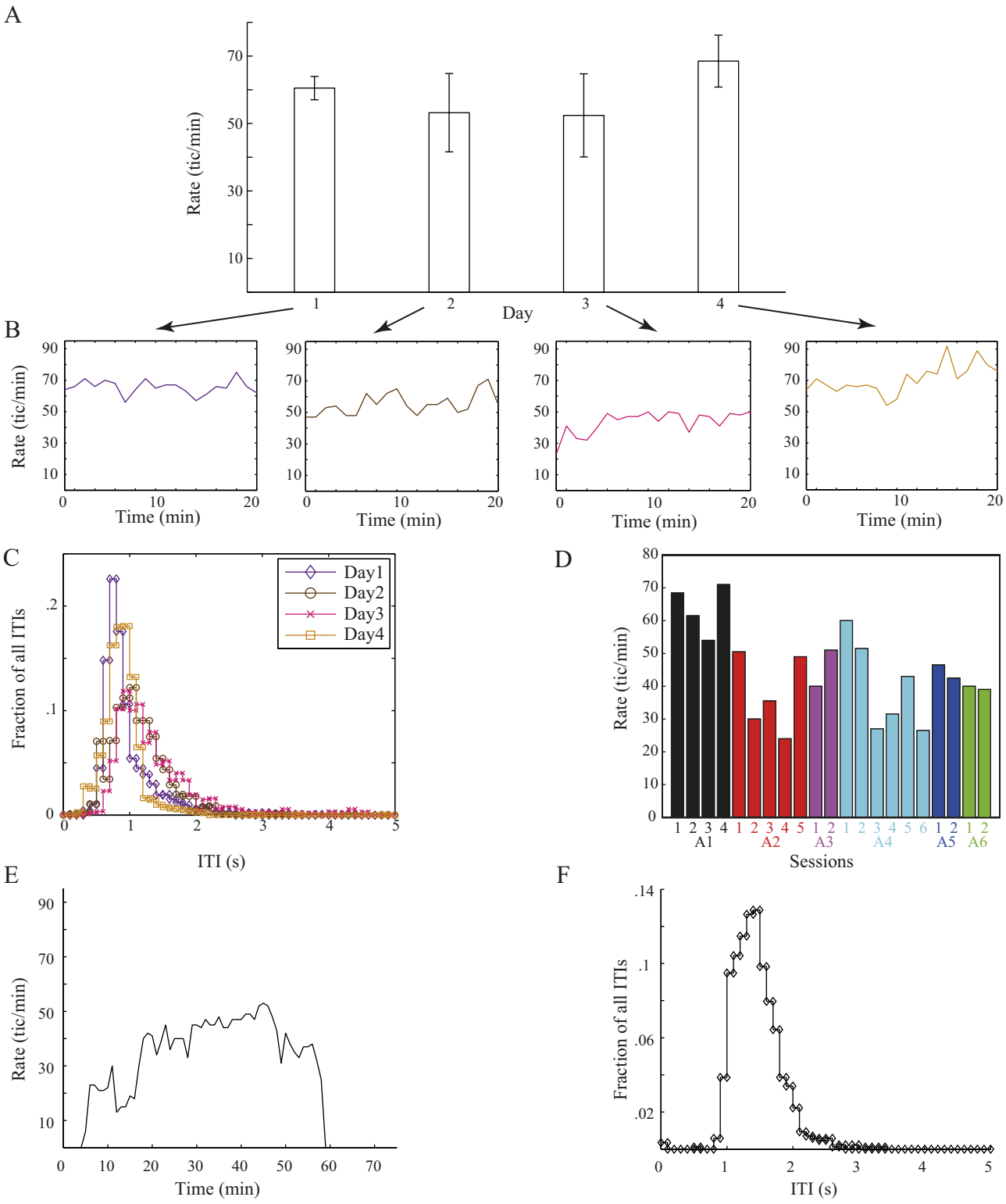

Fig. 3. Tic expression over multiple timeframes. (A) An example of the tic rate in the chronic model over 4 consecutive days of continuous bicuculline infusion (single animal). (B) Timeline of the changes in tic rate taken from 20 min periods within each day presented in *(A)*. (C) Histogram of the inter-tic intervals (ITIs) taken from the sessions presented in *(B)*. (D) Tic rate during multiple sessions, across all 6 animals (A1-6). (E-F) An example of the transient period of tic expression obtained from the acute model (single session). (E) Tic rate of an entire session, time 0 denotes the bicuculline injection. (F) ITI histogram of the steady state period (20–40 min post injection).

related changes in their activity (Fig. 4A). These changes consisted of excitation which could appear in 3 phases: early (0–50 ms), intermediate (50–200 ms) or late (200–350 ms), and inhibition which only occurred during the intermediate phase of the response. Most of the SPNs displayed early excitation (80%) and/or intermediate inhibition (76%); without any late response (Fig. 5B). FSIs presented varied response combinations which mostly included a decreased firing rate in the intermediate phase (92%). The neural response of the GP cells occurred primarily in the intermediate phase (85%), when 31% displayed excitation and 54% displayed inhibition of

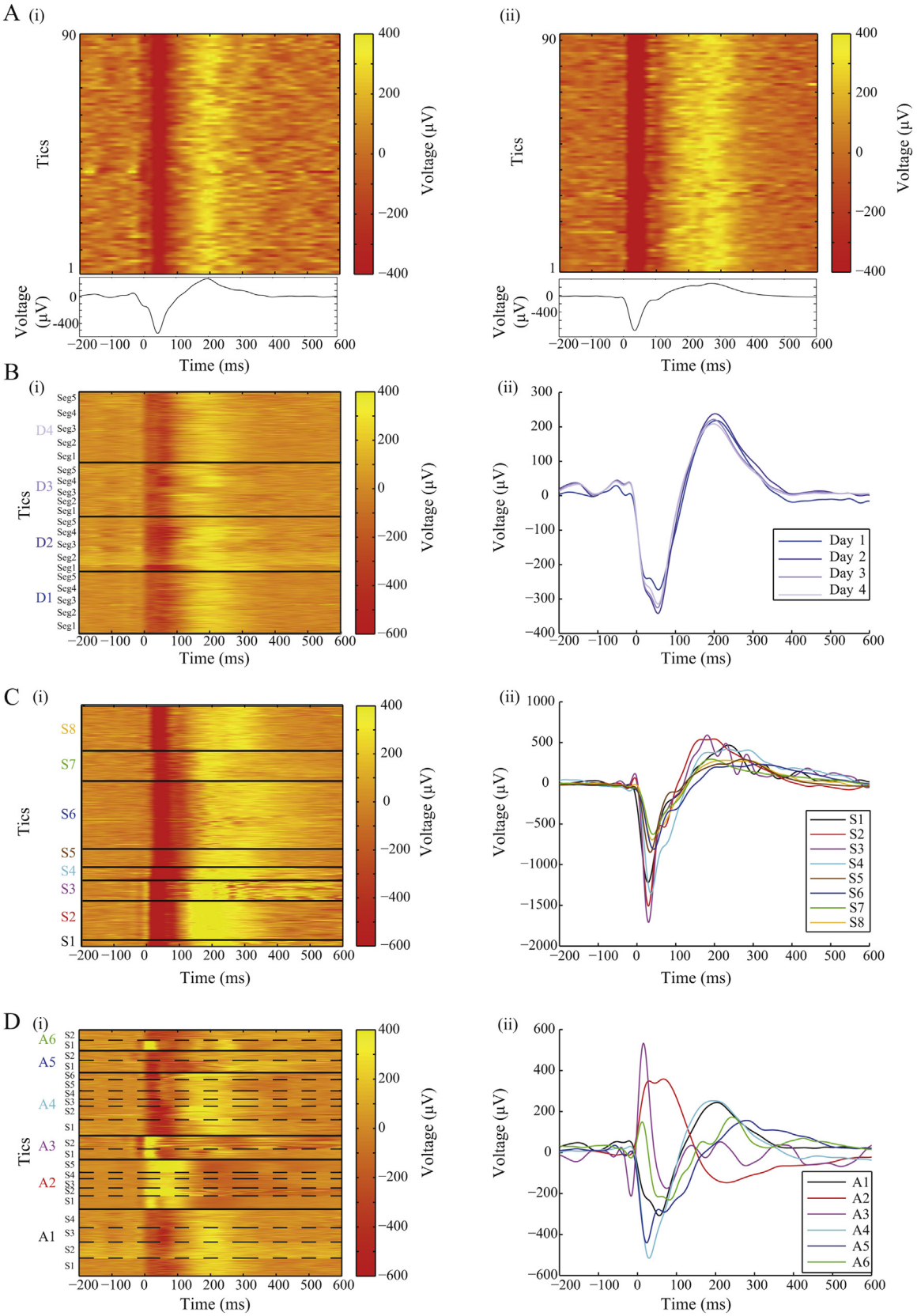

Fig. 4. Tic-associated LFP spikes. (A) Peri-tic LFP spikes of the (i, top) chronic and (ii, top) acute models over a short period in a single session, and the mean LFP spike shape for both sessions (bottom). (B) (i) Peri-tic LFP spikes and (ii) their mean shape obtained from a single chronic animal throughout multiple segments (Seg#) on 4 consecutive days (D#) (same example presented in Fig. 3A). (C) (i) Peri-tic LFP spikes and (ii) their mean shape taken from a single animal during different sessions (S#) (experimental days) of acute bicuculline injections. (D) (i) Peri-tic LFP spikes and (ii) their mean shape across multiple sessions and animals (A#) of the chronic model.(For interpretation of the references to colour in this figure legend, the reader is referred to the web version of this article.)

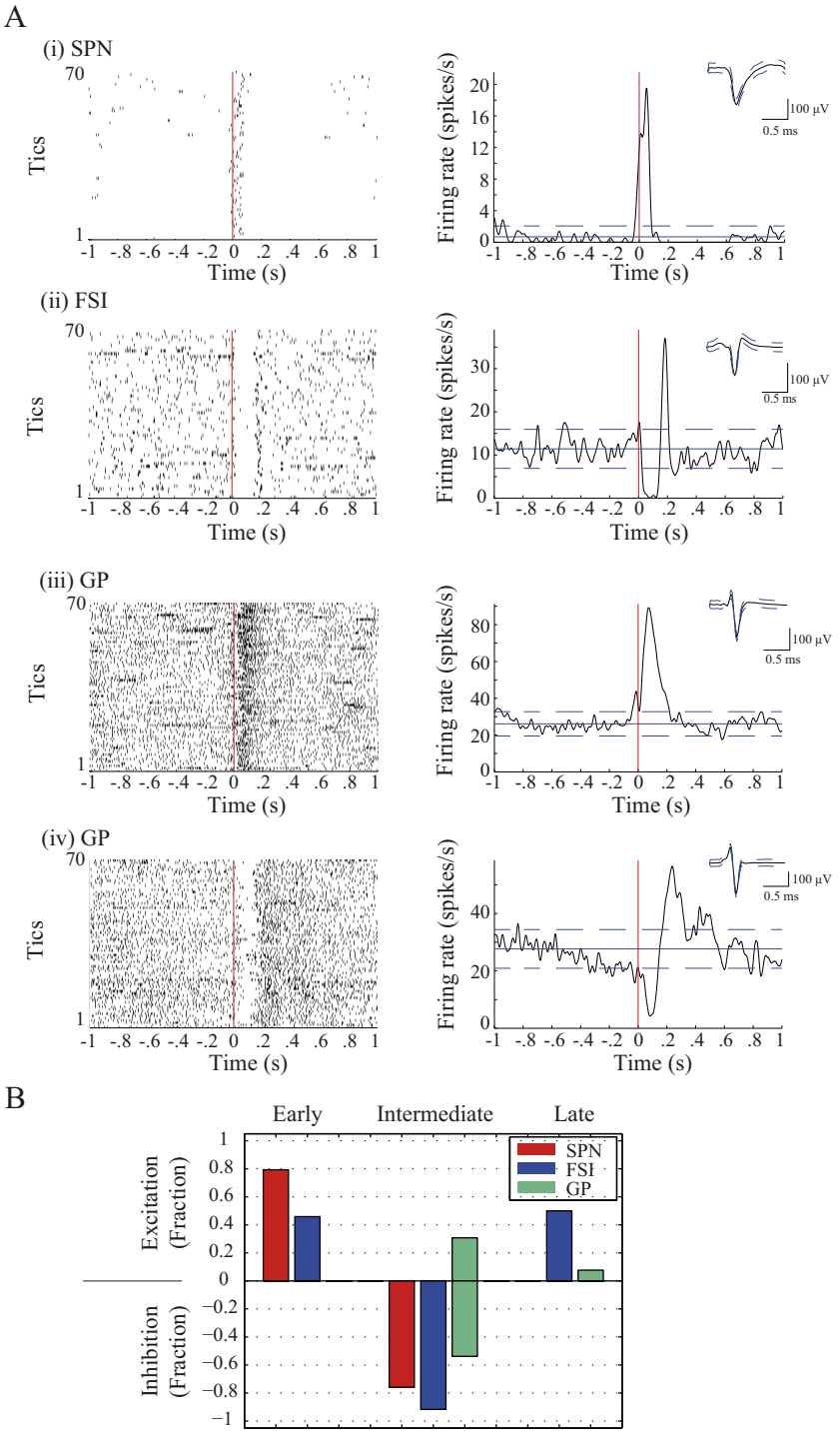

Fig. 5. Tic-related neural activity. (A) Peri-tic raster (left) and histogram (right) of (i) SPN, (ii) FSI and (iii, iv) GP neurons. The red vertical line marks the tic onset time and the blue horizontal lines mark the mean firing rate (solid) ± 2 SDs (dotted). The mean waveform of each neuron (solid) ± 1 SD (dotted) appears in the inset. (B) The percentage of neuronal responses during 3 phases: early (left), intermediate (middle) and late (right). (For interpretation of the references to colour in this figure legend, the reader is referred to the web version of this article.)

the firing rate. None of the neuronal populations displayed firing changes which were not temporally aligned to the tic execution and which may have been attributed to additional factors such as premonitory urges.

The chronic model facilitated prolonged experiments which enabled the comparison of the activity of individual neurons over multiple sessions within and between days. These recordings revealed that the neuronal activity around the tic time, which is stereotypic over short time scales (Fig. 6A–B), is stable across multiple days (Fig. 6C–D). Neuron stability across days was assessed by the preservation of the spike waveform, firing rate and pattern.

4. Discussion

In the current study, we presented a novel chronic model of tic expression in the rat, based on the striatal-disinhibition acute model (Bronfeld et al., 2013b; Israelashvili and Bar-Gad, 2015). Prolonged micro-infusion of $GABA_A$ antagonist (bicuculline) into the

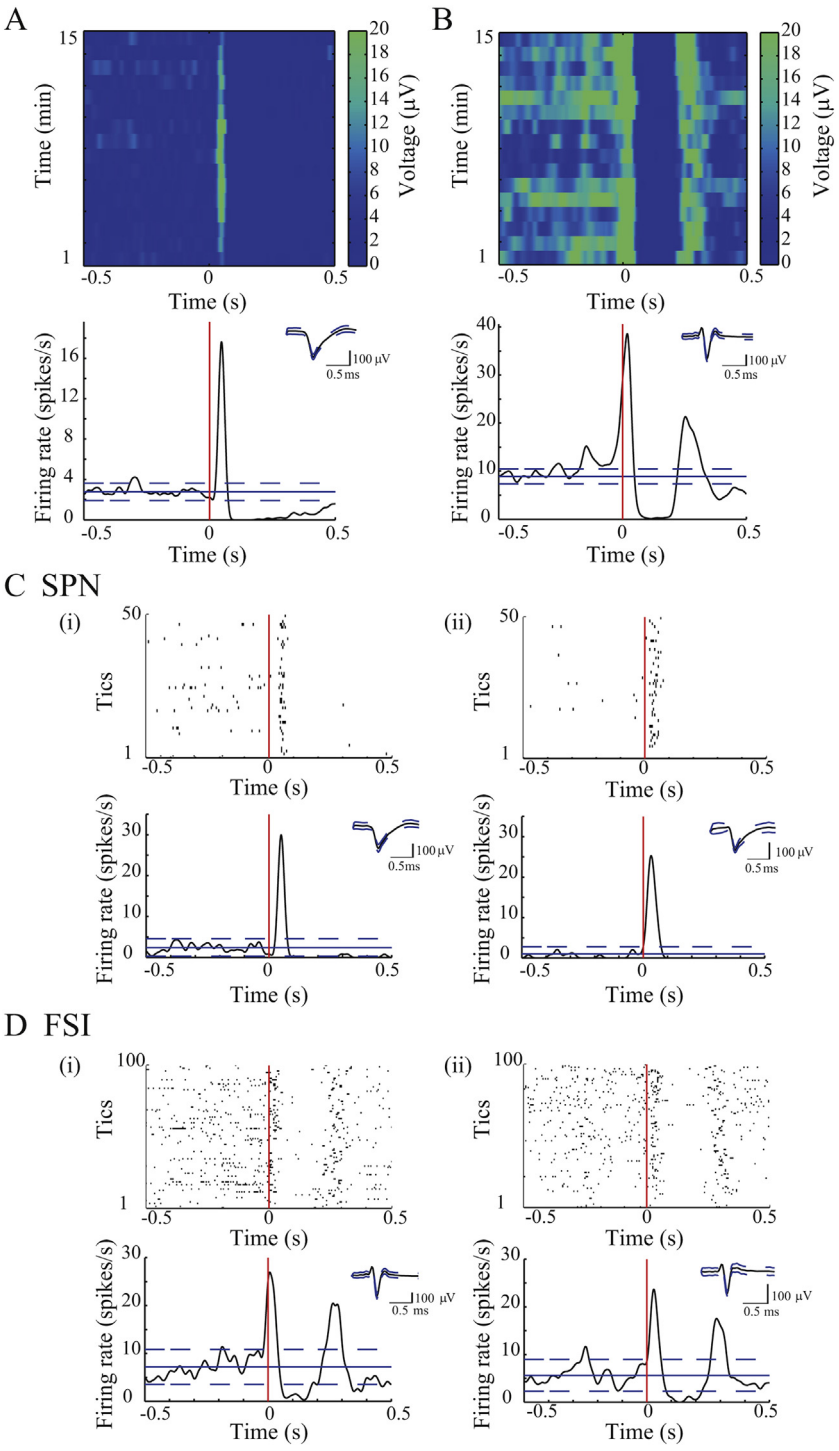

Fig. 6. Prolonged tic-related neural activity. (A–B) (i) Peri-tic time histogram and (ii) the mean peri-tic activity of (A) an SPN and (B) an FSI over a continuous 15 min period. The red vertical line marks the tic times and the blue horizontal lines mark the mean firing rate (solid) ± 2 SD (dotted). The mean waveform of the recorded neuron (solid) ± 1 SD (dotted) appears in the inset. (C-D) Peri-tic raster (top) and histogram (bottom) of the same SPN presented in *(A)* (C) and the same FSI presented in *(B)* during a single segment taken from 2 consecutive days. (For interpretation of the references to colour in this figure legend, the reader is referred to the web version of this article.)

dorsal striatum via a mini-osmotic pump led to ongoing expression of motor tics. Tic expression waxed and waned within a single day along with changes of the rat's behavioral state. However, during the waking state of the rat, tic properties such as type and frequency remained stable over multiple consecutive days. Electrophysiological recordings in the striatum and GP revealed the presence of LFP spikes, which have been shown to be highly correlated with individual tic expression in the acute model. The properties of the LFP spikes, such as shape and amplitude, were similar across different sessions and days within the same animal, but were different across animals. LFP spikes detection supplements two direct tic detection methods: Video based tic detection has low temporal accuracy (limited by the video rate) and depends on the magnitude of tic, additional movements of the animal and the location of the tic relative to the camera. Electromyography (EMG) provides high temporal and spatial resolution, but since tics are expressed in

multiple muscle groups, only implantation of multiple EMG electrodes will suffice in order to detect all the movements, which significantly burdens the well-being of the chronic model rats. LFP spike detection provides surrogate data which is highly correlated to the tics (McCairn et al., 2009; Israelashvili and Bar-Gad, 2015). In addition to the LFP spikes, tic-related changes were found in the activity of the majority of neurons in both nuclei. The neuronal activity changes typically appeared around the time of the onset of the motor tic, and presented heterogeneity which resembled the diversity seen in the acute model (McCairn et al., 2009; Israelashvili and Bar-Gad, 2015). The ongoing tic expression enabled prolonged recording periods, which demonstrated the stability of the LFP spikes and tic-related neural activity over timescales ranging from minutes to days. Identifying the same neuron across multiple days or even recording sessions is a major challenge in in-vivo extracellular electrophysiological experiments. However, it is likely to assume that the preservation of the neural properties, such as spike waveform and firing rate and pattern across days, indicates the stability of the same neural unit. The chronic striatal disinhibition model utilizes the two primary features of the acute model: a similar injected pharmacological agent (bicuculline) and a similar injection target (the dorsal striatum). Thus, the chronic model led to the expression of behaviorally similar motor tics and to the occurrence of similar tic-related LFP spikes and neural activity changes. However, the LFP spike properties in the chronic model were more stable across sessions within the same animal than in the acute model. This may be explained by the technical differences between the models: the chronic pump implantation limits variability within animals, due to the implantation of a single reservoir with a fixed rate infusion and target. In the acute model, the preparation of the injected material is done at the start of each session, which may lead to variability in injection properties such as concentration, volume and propagation radius. Furthermore, reinserting the injection cannula during each session leads to differences in the exact target location between acute sessions.

The chronic model utilizes osmotic pumps which are commonly used in a wide range of research fields. In our application, the optimal timeline for the chronic model manipulation included an initial ACSF mini-pump implantation, leading to multi-day ACSF infusion which was consequently replaced by a mini-pump containing bicuculline. This enabled the rats to fully recover from the surgery prior to tic initiation and avoided the potential stress caused by the combination of a brain surgery and an immediate continuous tic expression state. ACSF delivery is useful for generating a tic-free period, which can then serve as control neuronal recordings and behavioral monitoring. The subsequent bicuculline infusion is obtained by a simpler procedure of pump replacement and its attachment to the same implanted catheter, by opening the subcutaneously pocket on the rat's back and suturing it again. The bicuculline infusion period is dependent on the size and rate of the pump, which ranges from 1 day to 6 weeks. During this period tics typically appear continuously; however, several limitations may occur: prolonged infusion periods may cause brain tissue damage which may make it impossible to investigate the influence of the infused agent. Although no such damage was evident in the current study, it might play a role in the case of longer exposures. Second, detachment of the connection points may occur due to technical failure, greater movement and/or extensive grooming of the rat in the sutured area.

The chronic model upholds both construct validity and face validity. Its construct validity is based on its similarity to the etiology of the pathological state: imaging and postmortem evidence link the decreased binding of $GABA_A$ receptors and the numerical reduction of GABAergic interneurons in the striatum to the pathophysiology of tic disorders (Kalanithi et al., 2005; Kataoka et al., 2010; Lerner et al., 2012). This pathophysiology is imitated by the local infusion of the $GABA_A$ antagonist into the striatum, which causes over-activation of a focal striatal area pinpointed in theoretical models of the pathological changes occurring during the disorder (Mink, 2001 Albin and Mink, 2006). The chronic model displays motor tics that are similar to those seen in the acute model and are comparable to those observed in TS patients, hence addressing the face validity which estimates the similarity of the behavioral symptoms (Bronfeld et al., 2013a). The novelty of the chronic model lies in its ability to test the predictive validity, which refers to the compatibility of the animal model's response to treatments of the disorder. The fixed delivery rate of the pump ensures that tic fluctuation in this model is not a result of changes in the bicuculline concentration; thus different behavioral protocols and pharmacological agents can be tested.

Pharmacological models of Tourette syndrome are based on the manipulation of neuromodulators such as dopamine. These models are typically transient in nature and are based on the immediate effect of the pharmaceutical application. Furthermore, while most of these models share some properties with Tourette syndrome patients they do not typically produce tics (Bronfeld et al., 2013a). Existing chronic animal models of TS are based on genetic manipulations, primarily in mice. Currently, the face validity of these models is limited, since the animals display comorbid behaviors such as hyper-locomotion, excessive grooming, stereotyped and perseverative behaviors, but not the main behavioral sign of TS – tics (Godar et al., 2014). The D1CT-7 mice model exhibits motor tics with juvenile onset; however its construct validity is not in line with the common perception of TS pathophysiology (Nordstrom and Burton, 2002).

The new chronic striatal disinhibition model provides a unique opportunity to explore previously inaccessible core questions in the study of TS. The applications of the model may be divided into two broad categories: testing the effect of various treatments (behavioral, pharmaceutical or medical device based) and shedding light on the natural time course of the disorder. The effect of current treatments for TS: such as behavioral, feedback based, pharmaceutical, dopaminergic based, or medical devices, deep brain stimulation (DBS) based, all have a progressive effect on the expression of tics. The chronic model provides the ability to quantitatively test the evolving changes derived from the treatment. Unraveling the mechanism of tic fluctuation over different time scales requires a stable long-term model too. Clinical evidence links tic fluctuations to three main factors: willful tic suppression, internal behavioral states and external environmental factors. TS patients report that they can suppress their tics over short periods of time (minutes to hours) (Banaschewski and Rothenberger, 2003; Meidinger et al., 2005). Reinforcing tic suppression was shown to enhance tic reduction (Woods and Himle, 2004). Thus, the chronic model may be used for examining the modulation of reward on tic expression by operant learning. Internal behavioral states such as anxiety, fatigue, and concentration, as well as external environmental factors such as rich or stressful environment may also effect tic fluctuation (Silva et al., 1995; Conelea et al., 2011; Leckman et al., 2014). The ongoing tic expression in the chronic rat, enables the study of both the natural changes in tic expression during the shift between internal behaviors and the modulation of tic expression by external factors, such as stress manipulation. Based on findings from the acute model, the chronic model can also be used for studying different comorbidities of TS by altering the injection location within the striatum. Local injection in the dorsal striatum (sensorimotor area) was reported to lead to generation of motor tics and/or hyperactivity (Tarsy et al., 1978; McCairn et al., 2009; Worbe et al., 2009), whereas ventral striatum injections (associative and limbic areas) led to vocal tics or stereotyped behavior (Worbe et al., 2009; McCairn et al., 2016). Prolonged infusion in those areas may provide a better understanding of the development and the inter-

action of tics with other psychiatric behaviors. This model may thus accommodate the modifications needed for different studies: the implantation area can be changed according to the specific goal, larger pumps for longer periods can be used and implantation during different animal developmental stages can be used to study the neurodevelopmental dynamics related to the disorder.

5. Conclusion

The novel chronic model of tic expression in the rat, based on the striatal-disinhibition acute model, provides a new method for studying questions that have technically eluded investigation. This model serves as a platform for studying the neural mechanisms underlying TS clinical symptoms and their fluctuation over time. The stability of the model makes it possible to examine long-term therapeutic, behavioral and pharmacological treatments.

Acknowledgments

This work was supported in part by an Israel Science foundation (ISF) grant (743-13) and a Tourette Syndrome Association (TSA) grant. The authors thank D. Michaelson and G. Yadid for their help with the mini-osmotic pumps and K. Belelovsky, D. Yael, O. Tahary, L. Warhaftig and R. Plen for technical assistance.

Appendix A. Supplementary data

Supplementary data associated with this article can be found, in the online version, at http://dx.doi.org/10.1016/j.jneumeth.2017.03.003.

References

Abelson, J.F., et al., 2005. Sequence variants in SLITRK1 are associated with Tourette's syndrome. Science (80) 310, 317–320.
Albin, R.L., Mink, J.W., 2006. Recent advances in Tourette syndrome research. Trends Neurosci. 29, 175–182.
American Psychiatric Association, 2013. DSM-5.
Banaschewski, T., Rothenberger, A., 2003. Premonitory sensory phenomena and suppressibility of tics in Tourette syndrome: developmental aspects in children and adolescents. Dev. Psychopathol., 700–703.
Baym, C.L., Corbett, B.A., Wright, S.B., Bunge, S.A., 2008. Neural correlates of tic severity and cognitive control in children with Tourette syndrome. Brain 131, 165–179.
Bronfeld, M., Belelovsky, K., Bar-Gad, I., 2011. Spatial and temporal properties of tic-related neuronal activity in the cortico-basal ganglia loop. J. Neurosci. 31, 8713–8721.
Bronfeld, M., Israelashvili, M., Bar-Gad, I., 2013a. Pharmacological animal models of Tourette syndrome. Neurosci. Biobehav. Rev. 37, 1101–1119.
Bronfeld, M., Yael, D., Belelovsky, K., Bar-Gad, I., 2013b. Motor tics evoked by striatal disinhibition in the rat. Front. Syst. Neurosci. 7 (50).
Conelea, C., Woods, D.W., Brandt, B.C., 2011. The impact of a stress induction task on tic frequencies in youth with Tourette Syndrome. Behav. Res. Ther. 49, 492–497.
Gervasoni, D., Lin, S., Riberio, S., Soares, E., Pantoja, J., Nicolelis, M.A.L., 2004. Global forebrain dynamics predict rat behavioral states and their transitions. J. Neurosci. 24, 11137–11147.
Godar, S.C., Mosher, L.J., Di Giovanni, G., Bortolato, M., 2014. Animal models of tic disorders: a translational perspective. J. Neurosci. Methods 238, 54–69.
Israelashvili, M., Bar-Gad, I., 2015. Corticostriatal divergent function in determining the temporal and spatial properties of motor tics. J. Neurosci. 35, 16340–16351.
Kalanithi, P.S.A., Zheng, W., Kataoka, Y., DiFiglia, M., Grantz, H., Saper, C.B., Schwartz, M.L., Leckman, J.F., Vaccarino, F.M., 2005. Altered parvalbumin-positive neuron distribution in basal ganglia of individuals with Tourette syndrome. Proc. Natl. Acad. Sci. U. S. A. 102, 13307–13312.
Kataoka, Y., Kalanithi, P.S.A., Grantz, H., Schwartz, M.L., Saper, C., Leckman, J.F., Vaccarino, F.M., 2010. Decreased number of parvalbumin and cholinergic interneurons in the striatum of individuals with Tourette syndrome. J. Comp. Neurol. 518, 277–291.
Leckman, Zhang, H., Vitale, A., Lahnin, F., Lynch, K., Bondi, C., Kim, Y.S., Peterson, B.S., 1998. Course of tic severity in Tourette syndrome: the first two decades. Pediatrics 102, 14–19.
Leckman, J.F., Vaccarino, F.M., Kalanithi, P.S., Rothenberger, A., 2006. Annotation: tourette syndrome: a relentless drumbeat–driven by misguided brain oscillations. J. Child Psychol. Psychiatry 47, 537–550.
Leckman, J.F., King, R., Bloch, M.H., 2014. Clinical features of Tourette syndrome and tic disorders. J. Obsess. Compuls Relat. Disord. 3, 372–379.
Lerner, A., Bagic, A., Simmons, J.M., Mari, Z., Bonne, O., Xu, B., Kazuba, D., Herscovitch, P., Carson, R.E., Murphy, D.L., Drevets, W.C., Hallett, M., 2012. Widespread abnormality of the γ-aminobutyric acid-ergic system in Tourette syndrome. Brain 135, 1926–1936.
Mallet, N., Micklem, B.R., Henny, P., Brown, M.T., Williams, C., Bolam, J.P., Nakamura, K.C., Magill, P.J., 2012. Dichotomous organization of the external globus pallidus. Neuron 74, 1075–1086.
Marsden, C.D., Meldrum, B.S., Pycock, C., Tarsy, D., 1975. Focal myoclonus produced by injection of picrotoxin into the caudate nucleus of the rat. J. Physiol. 246 (96P).
McCairn, K.W., Bronfeld, M., Belelovsky, K., Bar-Gad, I., 2009. The neurophysiological correlates of motor tics following focal striatal disinhibition. Brain 132, 2125–2138.
McCairn, K.W., Nagai, Y., Hori, Y., Ninomiya, T., Kikuchi, E., Lee, J.-Y., Suhara, T., Iriki, A., Minamimoto, T., Takada, M., Isoda, M., Matsumoto, M., 2016. A primary role for nucleus accumbens and related limbic network in vocal tics. Neuron 89, 300–307.
McNaught, K.S.P., Mink, J.W., 2011. Advances in understanding and treatment of Tourette syndrome. Nat. Rev. Neurol. 7, 667–676.
Meidinger, A.L., Miltenberger, R.G., Himle, M., Omvig, M., Trainor, C., Crosby, R., 2005. An investigation of tic suppression and the rebound effect in Tourette's disorder. Behav. Modif. 29, 716–745.
Mink, J.W., 2001. Basal ganglia dysfunction in Tourette's syndrome: a new hypothesis. Pediatr. Neurol. 25, 190–198.
Morton, D.B., Griffiths, P.H.M., 1985. Guidelines on the recognition of pain, distress and discomfort in experimental animals and an hypothesis for assessment. Vet. Record (116), 431–436.
Muramatsu, S., Yoshida, M., Nakamura, S., 1990. Electrophysiological study of dyskinesia produced by microinjection of picrotoxin into the striatum of the rat. Neurosci. Res. 7, 369–380.
Nordstrom, E.J., Burton, F.H., 2002. A transgenic model of comorbid Tourette's syndrome and obsessive-compulsive disorder circuitry. Mol. Psychiatry 7, 617–625.
Paxinos, G., Watson, C., 2007. The Rat Brain in Stereotaxic Coordinates.
Peterson, B.S., Thomas, P., Kane, M.J., Scahill, L., Zhang, H., Bronen, R., King, R.A., Leckman, J.F., Staib, L., 2003. Basal ganglia volumes in patients with Gilles de la Tourette syndrome. Arch. Gen. Psychiatry 60, 415–424.
Pogorelov, V., Xu, M., Smith, H.R., Buchanan, G.F., Pittenger, C., 2015. Corticostriatal interactions in the generation of tic-like behaviors after local striatal disinhibition. Exp. Neurol. 265, 122–128.
Preston, R.J., Bishop, G.A., Kitai, S.T., 1980. Medium spiny neuron projection from the rat striatum: an intracellular horseradish peroxidase study. Brain Res. 183, 253–263.
Scharmann, W., 1999. Physiological and ethological aspects of the assessment of pain, distress and suffering. Hum. Endpoints Anim. Exp. Biomed. Res., 33–39.
Silva, R.R., Munoz, D.M., Barickman, J., Friedhoff, A.J., 1995. Environmental factors and related fluctuation of symptoms in children and adolescents with Tourette's disorder. J. Child Psychol. Psychiatry 36, 305–312.
Singer, H.S., Minzer, K., 2003. Neurobiology of Tourette's syndrome: concepts of neuroanatomic localization and neurochemical abnormalities. Brain Dev. 25, S70–S84.
Tarsy, D., Pycock, C.J., Meldrum, B.S., Marsden, C.D., 1978. Focal contralateral myoclonus produced by inhibition of GABA action in the caudate nucleus of rats. Brain 101, 143–162.
Tepper, J.M., Koós, T., Wilson, C.J., 2004. GABAergic microcircuits in the neostriatum. Trends Neurosci. 27, 662–669.
Woods, D.W., Himle, M.B., 2004. Creating tic suppression: comparing the effects of verbal instruction to differential reinforcement. J. Appl. Behav. Anal. 37, 417–420.
Worbe, Y., Baup, N., Grabli, D., Chaigneau, M., Mounayar, S., McCairn, K., Féger, J., Tremblay, L., 2009. Behavioral and movement disorders induced by local inhibitory dysfunction in primate striatum. Cereb. Cortex 19, 1844–1856.
Yael, D., Zeef, D.H., Sand, D., Moran, A., Katz, D.B., Cohen, D., Temel, Y., Bar-Gad, I., 2013. Haloperidol-induced changes in neuronal activity in the striatum of the freely moving rat. Front. Syst. Neurosci. 7, 110.